A Micro-Watt Metal-Insulator-Solution-Transport (MIST) Device for Scalable Digital Bio-Microfluidic Systems

R.B. Fair, M.G. Pollack, R. Woo, V.K. Pamula, R. Hong, T. Zhang, and J. Venkatraman
Department of Electrical and Computer Engineering
Duke University, Durham, N.C. 27708 USA

Abstract

In this work new data, models, and applications are presented of an ultra-low power, microfluidic device for use in integrated bio-microelectrofluidic systems (Bio-MEFS). The metal-insulator-solution transport (MIST) device is based on the high-speed manipulation of discrete droplets of analytes and reagents under voltage control, and is the MOSFET equivalent for MEFS.

Introduction

In recent years, a major research effort has been directed towards the miniaturization of biomedical laboratory instrumentation with a view towards creating highly integrated and automated "lab-on-a-chip" systems. Such systems critically depend on the ability to manipulate minute quantities of liquids rapidly and automatically. At present, most microfluidic systems utilize enclosed channels etched in glass or silicon through which liquid is pumped either mechanically or electrokinetically. However, these systems suffer from a number of drawbacks, including complex fabrication, slow inter-sample mixing and diffusion, high voltage or pressure requirements, valves with large dead volumes, and complex heterogeneous integration issues and control complexities.

Microfluidic systems based upon manipulation of discrete microdroplets within open structures are a promising alternative to conventional continuous flow systems. A number of methods for manipulating microdroplets based on direct electrical control have been proposed including dielectrophoresis [1], structured surfaces [2], thermocapillary [3,4], electrostatic [5,6], electrochemical [7] and photochemical effects [8].

We present here a method of transporting and manipulating microdroplets based upon direct electrical control of surface tension. We have demonstrated high speed transport of nl to µl volumes of droplets across two-dimensional arrays of electrodes. We also present new data, models, and applications of an ultra-low power, microfluidic device for use in integrated bio-microelectrofluidic systems (Bio-MEFS). The metal-insulator-solution transport (MIST) device is based on charge-control manipulation at the solution/insulator interface of discrete droplets by applting voltage to a control electrode. The MIST is the MOSFET equivalent for MEFS.

Background

A cross-section of a MIST device is shown in Fig. 1. A droplet is contained between two glass plates. An electrode pattern is etched on the bottom plate, which is then covered with a hydrophobic insulator. The top plate has a metal ground plane and is also coated with a thin insulator. Application of a gate voltage to an electrode above a threshold voltage initiates a contact angle change in the droplet, causing it to wet the area above the electrode. Sequential clock voltages applied to electrodes cause droplet transport at velocities up to 12 cm/sec. For 5 nano-liter droplets, a clock signal exceeding 1kHz has been tested. Plots of droplet velocity as a function of gate voltage are shown in Fig. 2 for four different electrode pitches.
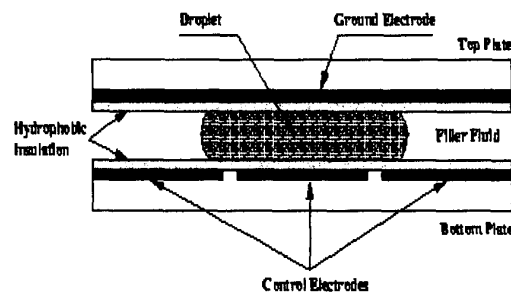

Fig. 1. Cross-section of electrowetting MIST device

Like the MOSFET, the MIST exhibits bilateral transport, is electrically isolated, uses a gate electrode for charge-controlled transport, has a threshold voltage, and is a square-law device in the relation between droplet velocity and gate actuation voltage.

New Droplet Velocity Model

We have developed a model for droplet actuation velocity based upon a statistical-molecular-interaction model, electrowetting theory, hydrodynamic dissipation, and surface tension imbalance at the droplet's contact line at the insulator surface. The 3D droplet transport problem has been reduced to a 2D problem with the cylindrical

16.4.1

geometry of Figs. 1 and 3. The driving force for transport, F_m, Occurs when a voltage is applied to an adjacent electrode. Staring with Young's and Lippman's equations [9], the expression for F_m is a function of the applied voltage, V:

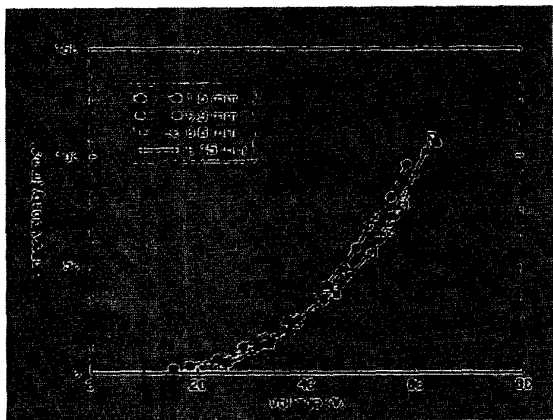$$F_m = \frac{\varepsilon_0 \varepsilon_R}{2d}(V - V_T)^2 \qquad (1)$$

Fig. 2. Droplet velocity vs. gate voltage for MIST devices with four electrode pitches. Over a 10-fold variation in pitch and a 300-fold variation in droplet volume, the velocity vs.voltage relationship holds. 0.1M KClsolution in 1 cSt. viscosity silicon oil.

where V is the gate voltage, V_T is the threshold voltage, and d is the thickness of the bottom dielectric layer in Fig. 1. The threshold voltage for transport is shown in Fig. 2 to be about 18V. The driving force, Fm, is balanced against the rate of dissipation in viscous flow and by dissipation by contact line friction. Thus, the transport kinetics of a droplet are governed by viscous dissipation in the core of a droplet and friction dissipation in the vicinity of the contact line, the capillary driving force being compensated for by the breaking force resulting from viscous shearing and contact line dragging. The derived expression predicts a square law between the actuation velocity and gate voltage divided by the friction coefficient $\zeta_0/2$ and viscous dissipation coefficient $3\mu L/h$. The identification of the dominating dissipation effect is through the relative magnitude of the ratio, R, of the two coefficients: $R = \zeta_0 h/6\mu L$. The average mass-transfer rate is:

$$U = \frac{\varepsilon_0 \varepsilon_R}{2d(\frac{\zeta_0}{2} + \frac{3\mu L}{h})}(V - V_T)^2 \qquad (2)$$

A diagram of the derived model is shown in Fig. 3. Initial justification of the model has been tested by successfully rationalizing experimental data for the effect of the droplet aspect ratio, L/h, and different electrode pitch sizes on droplet
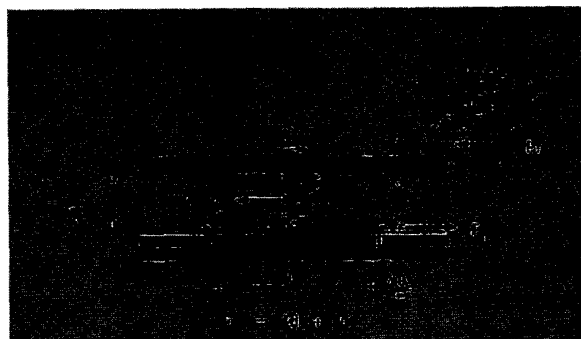
Fig. 3. Diagram of a model for droplet transport including hydrodynamic dissipation and surface tension imbalance during electrowetting actuation.

velocity. This investigation demonstrates that the droplet velocity is inversely proportional to the aspect ratio. However, for small aspect ratios, L/h, velocity is little affected by the change of aspect ratio, since friction is the main factor in determining the velocity. Thus, droplet velocity is relatively independent of the pitch size, as long as the aspect ratio small. Furthermore, the square law between velocity and voltage and the inverse proportion between viscosity and speed are also evident in the experiment. Finally, the consistency of the friction coefficient obtained from curve-fitting the experimental data with gap heights, h, varying from 0.19mm to 1.04mm, provide another validation of the model in Table 1. Table 1 was generated by fitting Eq. 2 to velocity data in which L=1.5mm and the droplet viscosity, μ=1cP. The table shows that the friction coefficient remains relatively constant for varying droplet aspect ratios, as does the threshold voltage, V_T.

TABLE I
EXTRACTED MODEL PARAMETERS FROM DATA

Gap Height (mm)	0.19	0.3	0.57	1.04
ζ_0	0.71	0.40	0.26	0.38
V_T (V)	16.8	16.9	16.9	17.0

Experimental

Chips were fabricated using standard microfabrication techniques. The control electrodes on the bottom plate were formed by patterning a single layer of 200nm thick chrome on a glass substrate with ~800nm parylene C deposited over the electrodes for insulation. The top-plate consisted of a plate of glass coated with a

16.4.2

conducting layer of optically transparent indium-tin-oxide (ITO). A very thin (~50 nm) layer of Teflon AF 1600 was applied as a top-coat to both top and bottom plates. The chips were assembled using a glass spacer to provide a fixed gap between the top and bottom plates. The top-plate electrode was grounded and a custom control system was used to independently switch each control electrode between ground and a dc voltage of up to 100 V.

We have performed high-speed capacitance measurements to characterize the electrowetting effect. Figure. 4b shows dynamic C-t data for a polar droplet moving across a linear array of three electrodes in air, and Fig. 4a shows data when the droplet is immersed in an oil medium. The initial spike in Fig. 4a is related to the trapping of oil beneath the droplet. From such measurements, we have determined that the peak instantaneous power required to actuate a 950 nano-liter water droplet is $1\mu W$, as is shown in Fig. 5.

capacitance are associated with spreading or motion of droplets. In addition to its value in fundamental studies, capacitance measurements may be practically utilized to monitor the position, speed or volume of microdroplets as they move through a system.

Fig. 5. Instantaneous power (200nW/div) vs. time (1 sec/div) needed to actuate a 950 nL droplet in oil with 50V gate voltage pulse.

Applications and Results

Side and top view images of droplet transfer between two adjacent electrodes in a linear array are shown in Fig. 6. The electrode pitch is 1.5 mm, the plate (gap) spacing is 0.30 mm and the electrolyte droplet is 900 nl of 100 mM KCl solution. The medium surrounding the droplet is air (side-view images) or low-viscosity (~1 cSt) silicone oil (top-view images). A threshold voltage of 10 – 20 V in silicone oil and 40 – 50 V in air is typically required to initiate motion of the droplet. Once the threshold voltage is exceeded the droplet rapidly moves and aligns itself with the energized electrode.

The MIST used in a micro-array can be reconfigured to perform multiple tasks under computer control. With regard to mixing, we have discovered that drop-drop chemical mixing can occur in seconds under actuation conditions rather than in minutes by diffusion processes. This result is demonstrated in Fig. 7. Using the principle of fast drop-drop mixing, we have developed an interpolating binary mixing architecture that allows mixing in large ratios (up to 64:1) in a binary manner with a few mixing operations. An analog (continuous flow)-to-digital (droplet flow) converter has been tested and is shown in Fig. 8 for rapid generation of droplets from a reservoir or for sampling a continuous stream.
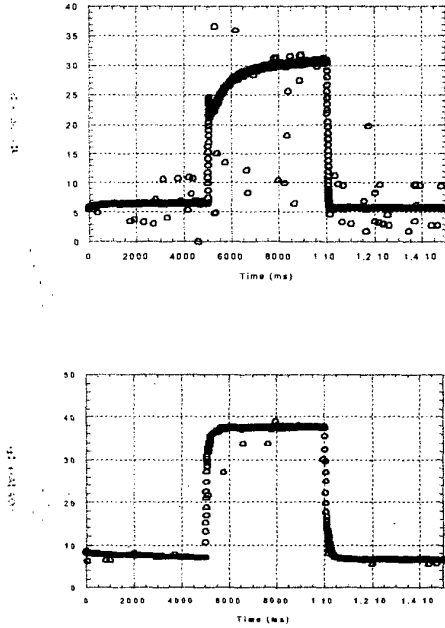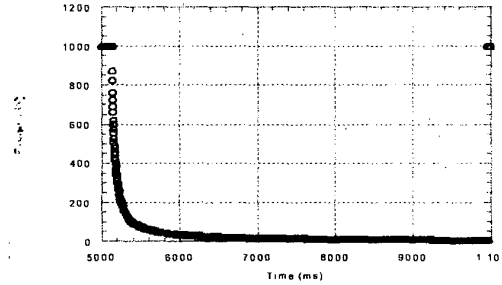
Fig. 4a (top). Dynamic capacitance vs. time data for a 950 nL 100mMKCL droplet being transported across a sensing electrode in a silicon oil medium; Vert: 5pF/div. Hor: 2 sec/div. Fig. 4b (below). C-t result in air. Vert: 10pF/div. Hor: 2 sec/div.

Dynamic measurement of the capacitance between the electrolyte droplet and underlying electrode is a convenient tool for studying electrowetting-based phenomena. Since electrowetting is inherently capacitive, large changes in
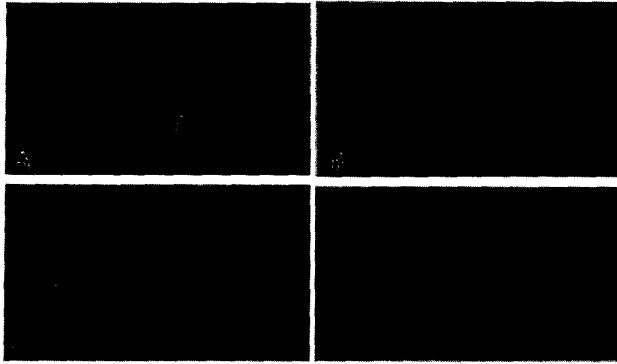
16.4.3

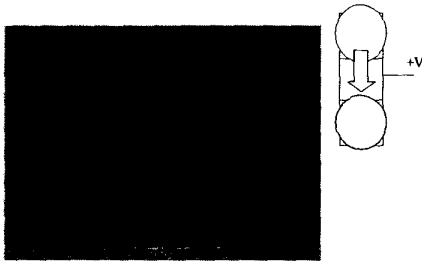Fig. 6. Side (A & B) and top (C & D) view time-lapse images of a droplet transfer (66 ms intervals)

Fig. 7. Graphic illustrating high speed mixing in seconds when a 1.5 uL water droplet is actuated into a 1.5 uL droplet containing fluorescein. Non-actuated mixing is diffusion controlled and requires 1-2 minutes.

Fig. 8. Time-lapsed series showing droplet formation from a continuous source of water in a pipette.

Automatic generation of uniform unit-sized microdroplets is a critical operation for realizing droplet-based microfluidic systems. Microdroplets may be formed either from a larger sample droplet or from a continuously-flowing sample stream. Microdroplet formation by electrowetting may be accomplished by alternately advancing and receding a liquid front across one or more energized electrodes. As the liquid front retracts, microdroplets remain behind in the surface-tension wells created by the energized electrodes. Since the electrode geometry and plate-spacing define the droplet shape, highly reproducible volumes can be obtained. When dispensing from an on-chip source, electrowetting may be used to form fingers or projections of a larger sample droplet which are subsequently "pinched-off" to form microdroplets by de-energizing one or more intermediate electrodes in the pathway. Another alternative is to use an external pressure source to drive the liquid front across the chip. In this case, pressurized liquid enters the chip through a hole in the top-plate. The liquid spreads within the gap between the plates and is subsequently retracted leading to the formation of single or multiple microdroplets at specified locations. Importantly, this arrangement provides an interface between continuous and discrete microfluidic systems (i.e. discretization).
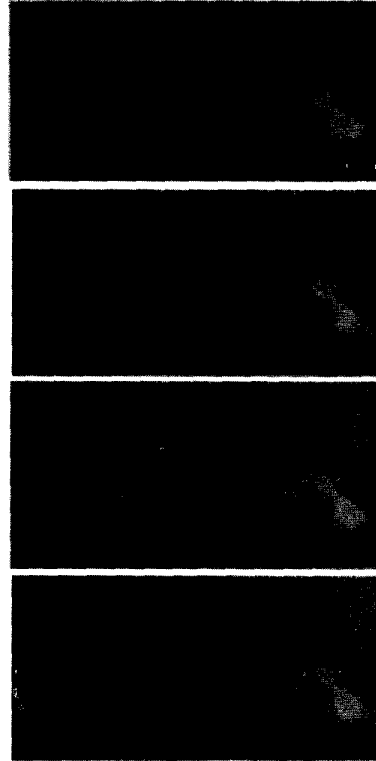
References

1] T.B. Jones, M. Gunji, M. Washizu, and M.J. Feldman, "Dielectrophoretic liquid actuation and nanodroplet formation," *J. Appl. Phys.*, vol. 89, pp. 1441-1448, 2001.

[2] O. Sandre, L. Gorre-Talini, A. Ajdari, J. Prost, and P. Silberzan, "Moving droplets on asymmetrically structured surfaces," *Phys. Rev. E*, vol. 60, pp.2964-2972, 1999.

[3] M.A. Burns et al., "Microfabricated structures for integrated DNA analysis," *Proc. Natl. Acad. Sci. USA*, vol. 93, pp. 5556-5561, 1996.

[4] T.S. Sammarco and M.A. Burns, "Thermocapillary pumping of discrete droplets in microfabricated analysis devices," *AIChe J.*, vol. 45, 350-366, 1999.

[5] M. Washizu, "Electrostatic actuation of liquid droplets for microreactor applications," *IEEE Trans. Ind. Appl.*, vol. 34, pp. 732-737, 1998.

[6] M.G. Pollack, R.B. Fair and A.D. Shenderov, "Electrowetting-based actuation of liquid droplets for microfluidic applications," *Appl. Phys. Lett.*, vol. 77, pp. 1725-1726, 2000.

[7] B.S. Gallardo et al., "Electrochemical principles for active control of liquids on submillimeter scales," *Science*, vol. 283, pp. 57-60, 1999.

[8] K. Ichimura, S. Oh, and M. Nakagawa, "Light-driven motion of liquids on a photoresponsive surface," *Science*, vol. 288, pp. 1624-1626, 2000.

[9] M. Schneemilch, W.J.J. Welters, R.A. Hayes, and J. Ralsoton, "Electrically Induced Changes in Dynamic Wettability," *Langmuir*, vol. 16, pp. 2924-2927, 2000.